

1
2
3
4
5
6
7
8
9
10
11
12
13
14
15
16
17
18
19
20
21
22
23
24
25
26
27
28
29
30
31
32
33
34
35
36
37
38
39
40
41
42
43
44
45
46
47
48
49
50
51
52
53
54
55
56
57
58
59
60

Online Data Supplement

Excess mucus viscosity and airway dehydration impact COPD airway clearance

Vivian Y. Lin, Niroop Kaza, Susan E. Birket, Harrison Kim, Lloyd J. Edwards, Jennifer LaFontaine, Linbo Liu, Marina Mazur, Liping Tang, Stephen A. Byzek, Justin Hanes, Guillermo J. Tearney, S. Vamsee Raju, Steven M. Rowe*

Extended Materials and Methods

Smoke exposure

Primary HBE cells were apically exposed to 2% cigarette smoke extract (CSE) [1] or DMSO vehicle (24 hr) prior to imaging. All cigarette smoke was generated from 3R4F cigarettes (University of Kentucky, Lexington, Kentucky, USA).

Standardized anesthesia and intubation protocol

Ferrets (0.6-1.8 kg in weight) were anesthetized with an IACUC-approved formulation of dexmedetomidine (0.4 mg/kg, IM) in combination with ketamine (2.8 mg/kg, IM).

Ophthalmic lubricant was applied to the eyes once sedation was achieved. The animals were placed on a heated operating table until recovery. Atipamezole was given as a reversal agent at an equal volume as the dexmedetomidine.

In vivo mucociliary clearance

Sedated ferrets were placed in nose-only restraint tubes similar to the ones used for smoke exposures for administration of ^{99}Tc . Regions of interest (ROI) corresponding to the entire left and right lungs were determined as indicated by concomitant chest radiograph, and counts measured and calculated after correction for radioactive decay. Results were expressed as percentage of radioactivity present in the initial baseline image. Data are plotted as retention of radioactivity vs. time for the whole lung.

Tissue preparation

1
2
3 Connective tissue was removed from excised tracheal and bronchial sections before
4 opening each along the non-cartilaginous tissue for imaging. Samples were incubated
5 at 37°C (5% CO₂) between imaging sessions. All agents were added to the basolateral
6 surface of the trachea (so as not to add exogenous fluid to the apical surface), and
7 stimulants were allowed to incubate for a sufficient duration (30 min) to impart their
8 effects. Indomethacin was used to avoid prostaglandin signaling as a mediator of
9 pharmacologic agents [2], while low-dose carbachol helped stimulate some epithelial
10 secretion for additional mucus transport measurements. Following these imaging
11 treatments, each ferret trachea was then treated with a combination of higher
12 concentration carbachol and phenylephrine, which was necessary to stimulate maximal
13 secretion (5-30 µL collected volume) for subsequent collection and use in mucus-related
14 assays.
15
16
17
18
19
20
21
22
23
24
25
26
27
28
29
30
31
32

33 *Micro-optical coherence tomography (µOCT) imaging*

34
35 This real-time system provides high-resolution, cross-sectional images of the airway
36 epithelial surface, thereby allowing for simultaneous quantification of airway surface
37 liquid (ASL) depth, periciliary layer (PCL) height, cilia beat frequency (CBF), and
38 mucociliary transport (MCT) rate in a co-localized fashion. Multiple ROI (2-4 per
39 transwell filter or at least 10 per trachea) were imaged to account for variability within
40 individual samples. Cells were imaged at baseline and 24 hr post-exposure.
41
42
43
44
45
46
47
48
49
50

51 *Particle tracking microrheology (PTM)*

52
53
54
55
56
57
58
59
60

1
2
3 Fluorescent beads were imaged using TRITC (500-nm) and GFP (1- μ m) channels in
4 the same ROI, and in the same or adjacent plane. 4-5 ROI were imaged per coverslip,
5
6 with 10-25 individual particles per ROI tracked using ImageJ SpotTracker (NIH); these
7
8 tracks were then sorted and analyzed using custom MatLab scripts to quantify mean-
9
10 squared displacement of particles over time, from which effective viscosity can be
11
12 calculated [3].
13
14
15
16
17
18
19

20 *Histological staining.*

21
22 Formalin-fixed human and ferret airway tissues were stained with hemotoxylin and
23
24 eosin (H&E) or Alcian blue/periodic acid-Schiff (AB/PAS), to assess smoke-induced
25
26 changes in morphology and mucus-producing structures, respectively.
27
28
29
30
31

32 *Statistical analysis.*

33
34 All groups of data were analyzed using the D'Agostino-Pearson normality test to
35
36 determine whether a parametric or non-parametric test should be used. Results for
37
38 airway microanatomy and viscoelasticity metrics between control and smoke-exposed
39
40 tissues over time were assessed by two-way ANOVA, and those between control and
41
42 COPD or smoke-exposed groups were compared using unpaired Mann-Whitney or t-
43
44 test. Wilcoxon was used to compare paired measures pre- and post-stimulation within
45
46 each exposure group. Correlations between metrics were calculated using linear or
47
48 semi-log regression methods. A univariate model was performed to assess for effects
49
50 on mean MCT. A linear mixed model for repeated measures analysis was used to
51
52 model MCT as a repeated measure (technical and biological replicates) using
53
54
55
56
57
58
59
60

1
2
3 previously published statistical methods [4, 5], and predictors included time effects,
4 cohort effects, sex effects, smoking effects, and the potential for interaction among
5 them. A separate linear mixed model was used to assess the relationship between MCT
6 and mean ASL, mean PCL, and mean CBF as independent variables along with time
7 category, smoking status, cohort, and sex. Random effects included intercept and
8 repeated measures at baseline, or random intercept only. Unstructured random effects
9 covariance matrix was used for each analysis. The final models omitted interaction
10 terms between predictor variables and time or cohort, as these were not significant and
11 did not alter conclusions. R^2 were estimated by previous methods [6].
12
13
14
15
16
17
18
19
20
21
22
23
24
25
26
27
28
29
30
31
32
33
34
35
36
37
38
39
40
41
42
43
44
45
46
47
48
49
50
51
52
53
54
55
56
57
58
59
60

Supplemental Tables

Table S1. Univariate linear regression analysis for mean MCT in steady-state conditions. By ferret (N=54).

Predictor	β	P-value	R²
Smoke	-3.09	< 0.028	0.089
CBF	1.34	< 0.007	0.129
PCL	0.530	0.608	0.005
ASL	-0.40	0.114	0.047
Female	-0.22	0.879	0.000

Table S2. Tissue donor demographics.

	Non-Smoker (n = 3)	Healthy Smoker (n = 6)	COPD (n = 3)
Gender	Female (1) Male (2)	Male (6)	Female (2) Male (1)
Age (years)	44 ± 19.8	44.5 ± 9.8	51.3 ± 9.1
Race	White (2) Black (1)	White (6)	White (1) Black (2)
Donors with emphysema	0	0	1
Smoking history (Pack-years)	N/A	34.3 ± 17.5	36.7 ± 29.3

Supplemental Figure Legends

Figure S1. Deposition of Tc⁹⁹-DTPA in ferret tissues. (A) Representative uncorrected images of Tc⁹⁹-DTPA deposition in the lungs acquired at baseline (Time 0). **(B)** Total deposition of radiolabel at Time 0 was quantified before assessment of clearance. **(C)** Systemic absorption of Tc⁹⁹-DTPA as monitored by uptake into forearm muscles.

Figure S2. Schematic of experimental protocol for ferret trachea. Upon euthanization, the trachea was removed from each animal and immediately dissected for μ OCT imaging, followed by cholinergic stimulation of mucus secretion for assessment of mucus properties such as microrheology and percent solids by weight. Thick borders indicate endpoint collection throughout the protocol. Capitalized words indicate key timepoints for endpoints. Abbreviations: μ OCT = micro-optical coherence tomography, PTM = particle tracking microrheology.

Figure S3. Distribution of μ OCT-quantified airway epithelial function by region of interest (ROI). μ OCT was used to measure **(A)** ASL depth, **(B)** PCL height, **(C)** CBF, and **(D)** MCT rate at multiple ROI per ferret trachea, to account for the local microenvironment. Data is presented as box-and-whisker (Tukey method). n = 1078 videos.

Figure S4. Cigarette smoke exposure reduces MCT in primary HBE cells. (A) Representative μ OCT stills of primary HBE cells after 24-hour apical treatment with 2% cigarette smoke extract (CSE) or DMSO control. Red line = ASL. Yellow line = PCL. **B-**

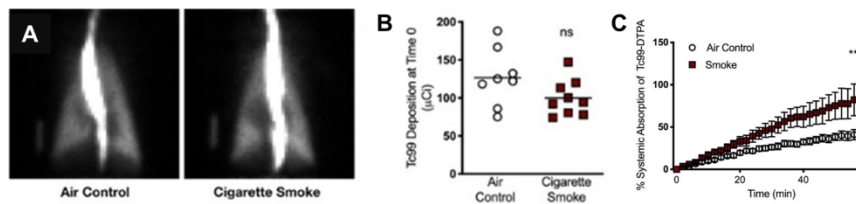
1
2
3 **C:** Quantification of *in vitro* ASL (**B**) and MCT (**C**) following exposure. $n = 10$ ROI, $**p <$
4
5 0.01 , $***p < 0.001$ compared to vehicle control, as determined by unpaired Mann-
6
7 Whitney (ASL) and t-test (MCT).
8
9

10
11
12 **Video S1.** Representative μ OCT video of mucus transport in a trachea excised from an
13
14 air control ferret.
15
16

17
18
19 **Video S2.** Representative μ OCT video of mucus transport in trachea from a smoke-
20
21 exposed ferret.
22
23

24 25 26 **References in Online Supplement**

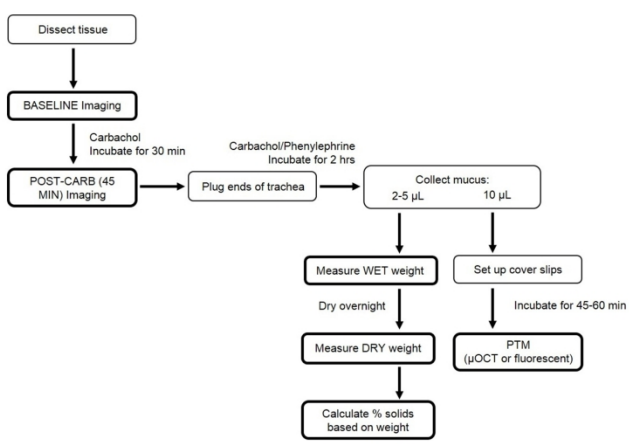
- 27
28 1. Raju SV, Lin VY, Liu L, McNicholas CM, Karki S, Sloane PA, Tang L, Jackson PL, Wang
29 W, Wilson L, Macon KJ, Mazur M, Kappes JC, DeLucas LJ, Barnes S, Kirk K, Tearney GJ,
30 Rowe SM. The Cystic Fibrosis Transmembrane Conductance Regulator Potentiator Ivacaftor
31 Augments Mucociliary Clearance Abrogating Cystic Fibrosis Transmembrane Conductance
32 Regulator Inhibition by Cigarette Smoke. *Am J Respir Cell Mol Biol* 2017; 56(1): 99-108.
- 33
34 2. Joo NS, Jeong JH, Cho HJ, Wine JJ. Marked increases in mucociliary clearance
35 produced by synergistic secretory agonists or inhibition of the epithelial sodium channel. *Sci*
36 *Rep* 2016; 6: 36806.
- 37
38 3. Chu KK, Mojahed D, Fernandez CM, Li Y, Liu L, Wilsterman EJ, Diephuis B, Birket SE,
39 Bowers H, Martin Solomon G, Schuster BS, Hanes J, Rowe SM, Tearney GJ. Particle-Tracking
40 Microrheology Using Micro-Optical Coherence Tomography. *Biophys J* 2016; 111(5): 1053-
41 1063.
- 42
43 4. Laird NM, Ware JH. Random-effects models for longitudinal data. *Biometrics* 1982:
44 38(4): 963-974.
- 45
46 5. Edwards LJ. Modern statistical techniques for the analysis of longitudinal data in
47 biomedical research. *Pediatr Pulmonol* 2000; 30(4): 330-344.
- 48
49 6. Edwards LJ, Muller KE, Wolfinger RD, Qaqish BF, Schabenberger O. An R2 statistic for
50 fixed effects in the linear mixed model. *Stat Med* 2008; 27(29): 6137-6157.
51
52
53
54
55
56
57
58
59
60



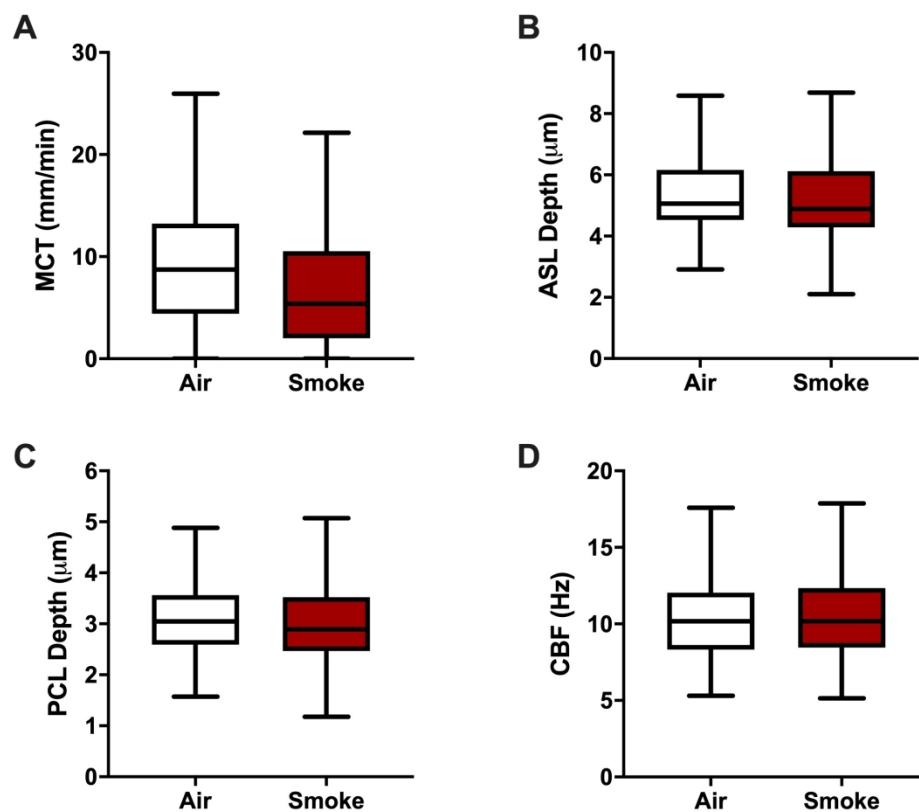
190x254mm (300 x 300 DPI)

1
2
3
4
5
6
7
8
9
10
11
12
13
14
15
16
17
18
19
20
21
22
23
24
25
26
27
28
29
30
31
32
33
34
35
36
37
38
39
40
41
42
43
44
45
46
47
48
49
50
51
52
53
54
55
56
57
58
59
60

1
2
3
4
5
6
7
8
9
10
11
12
13
14
15
16
17
18
19
20
21
22
23
24
25
26
27
28
29
30
31
32
33
34
35
36
37
38
39
40
41
42
43
44
45
46
47
48
49
50
51
52
53
54
55
56
57
58
59
60

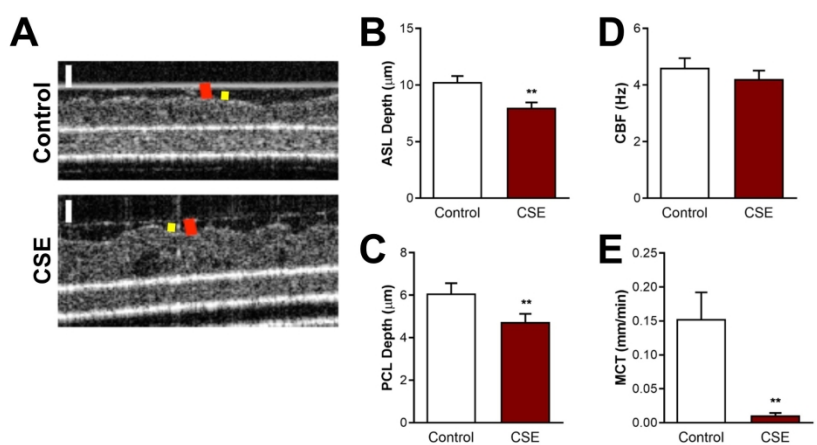


190x254mm (300 x 300 DPI)



191x160mm (300 x 300 DPI)

1
2
3
4
5
6
7
8
9
10
11
12
13
14
15
16
17
18
19
20
21
22
23
24
25
26
27
28
29
30
31
32
33
34
35
36
37
38
39
40
41
42
43
44
45
46
47
48
49
50
51
52
53
54
55
56
57
58
59
60



190x254mm (300 x 300 DPI)